Tunnelling and Underground Space Technology 30 (2012) 233–245

Contents lists available at SciVerse ScienceDirect

Tunnelling and Underground Space Technology

journal homepage: www.elsevier.com/locate/tust

Technical Note

Double-O-Tube shield tunneling for Taoyuan International Airport Access MRT

Yung-Show Fang [a,*], Chung-Cheng Kao [b], Yu-Fen Shiu [a]

[a] Department of Civil Engineering, National Chiao Tung University, Hsinchu, Taiwan
[b] Department of Rapid Transit Systems, Taipei City Government, Taipei, Taiwan

ARTICLE INFO

Article history:
Received 14 February 2011
Received in revised form 30 January 2012
Accepted 18 March 2012
Available online 12 April 2012

Keywords:
DOT tunneling
Settlement
Shield
Tunneling cost
Tunneling duration

ABSTRACT

From 1989 to 2010, 20 tunneling projects have been carried out with the Double-O-Tube (DOT) shield tunneling method in the world. In this paper, the DOT shield tunneling for the construction of Taoyuan International Airport Access (TIAA) Mass Rapid Transit (MRT) system is introduced. A 6.42 m-diameter, 11.62 m-wide DOT shield machine was used to build the first DOT tunnel in Taiwan. Field data indicated that, throughout the tunneling operation, the rolling angle of the DOT shield varied between +0.23° and −0.39°, which was within the limiting design values of +0.6° and −0.6° proposed by both TIAA MRT and Shanghai Metro. For the six surface settlement troughs collected from Tokyo, Shanghai and Taipei, the ground loss due to DOT shield tunneling ranged from 0.23% to 1.30%, and the average ground loss was 0.78%. As compared with the ground loss due to single-circular Earth-Pressure-Balance (EPB) shield tunneling in cohesive soils, the range of ground loss due to DOT shield tunneling was relatively narrow, and the peak ground loss value was significantly less. Underground excavation with the DOT tunneling method would increase the tunneling duration for about 32%. The cost per meter of tunnel constructed with a DOT shield was about 1.5 times that constructed with single-circular shields. The cost of shield machine and segment lining were 23% and 53% of the total tunneling costs respectively. The expensive DOT shield machine and the complicated manufacturing and assembly of DOT lining segments are the main reasons for higher cost of tunneling. However, it would cost a lot more budget and it would be much more risky to excavate three cross-passages between the single-circular tunnels under the river.

1. Introduction

In recent years, due to the rapid development of urban areas, a lot of public facilities such as the Mass Rapid Transit (MRT) systems and underground sewerage systems have been constructed. Because of the disruptive effects of the cut-and-cover method, it has been becoming more popular to employ the shield tunneling method for passing under commercial areas with heavy traffic. The Double-O-Tube (DOT) shield tunneling has a minimized section area, and enables the most efficient use of underground space (Chow, 2006). As compared with circular twin-tube tunnels, the DOT shield tunnel may pass narrow underground corridors, and the impact on nearby structures is minimized (Sterling, 1992; Moriya, 2000).

From 1989 to 2010, as summarized in Table 1, 20 tunneling projects were constructed with DOT shield tunneling method. The first 13 cases were carried out in Japan, the next six cases were conducted in Shanghai, China, and the latest one was constructed in Taipei, Taiwan. The purposes of tunneling were to excavate subway tunnels, sewer mains, and common conduits. The formation of soil consisted of gravel, sand, silt, clay and peat. In Table 1, the diameter of DOT shields varied from 4.45 to 9.36 m, and the width of shields varied from 7.65 to 15.86 m. The length of tunnel ranged from 249 to 2497 m. The minimum radius of curvature of tunnel alignment was 102 m, and the maximum tunnel gradient was 5.9%. Table 1 indicated, all 20 DOT shields used up to 2010 were made by Japanese manufactures. It is obvious that Japanese play a leading role regarding the development of DOT shield tunneling technology. In Table 1, IHI represents Ishikawajima-Harima Heavy Industries, MHI represents Mitsubishi Heavy Industries, and KHI represents Kawasaki Heavy Industries.

In this paper, the DOT shield tunneling for the construction of Taoyuan International Airport Access (TIAA) MRT is introduced. This is the first DOT shield machine employed in Taiwan. The rolling angle of the DOT shield measured as a function of the ring number was presented and studied. Surface settlement troughs due to DOT shield tunneling in Japan, Shanghai and Taipei were collected and compared with those estimated with empirical methods.

Shen et al. (2009) stated that the disadvantages for a single-circular shield tunnel are resulted by high construction cost and long construction period. That is why the DOT shield tunneling method was proposed in Japan. However, from a practical point

* Corresponding author. Tel.: +886 3 571 8636; fax: +886 3 571 6257.
E-mail address: ysfang@mail.nctu.edu.tw (Y.-S. Fang).

0886-7798/$ - see front matter © 2012 Elsevier Ltd. All rights reserved.
http://dx.doi.org/10.1016/j.tust.2012.03.001

Table 1
Projects constructed with DOT shield tunneling method.

Case no.	Project name	Purpose of tunnel	Geological condition	External dimensions of DOT shield (m)	Length of tunnel (m)	Thickness of overburden (m)	Minimum radius of curvature (m)	Maximum gradient (%)	DOT shield manufacture	Period of construction
1	Rijo tunnel, 54th national route Hiroshima, Japan	Subway	Clay, sand	∅6.09 × W10.69	850	5.0–8.3	135	1.8	IHI	1989–1994
2	Kikutagawa 2nd sewer main Narashino, Chiba, Japan	Sewer main	Fine sand, clay, peat	∅4.45 × W7.65	703	2.15–9.0	1600	4.0	IHI	1990–1994
3	Ariakekita common conduit Tokyo, Japan	Common conduit	Clay, gravel	∅9.36 × W15.86	249	14.0–17.0	1600	3.5	MHI	1990–1994
4	Underground line, coastline high speed transit, Kobe, Japan	Subway	Clay, gravel	∅5.48 × W9.75	304	11.5–15.5	1500	0.8	MHI	1995–1998
5	East district of Sunadahashi, 4th line high speed transit, Nagoya, Japan	Subway	Sandy gravel, silt, clay	∅6.52 × W11.12	752	10.31–16.6	500	2.3	IHI	1999–2002
6	Chayagasaka park district, 4th line, high speed transit, Nagoya, Japan	Subway	Silt, sand	∅6.52 × W11.12	1007	11.0–32.1	500	3.3	IHI	1999–2002
7	Yamamoto north district, 4th line, high speed transit, Nagoya, Japan	Subway	Clay, sand, sandy gravel	∅6.52 × W11.12	1238	9.3–32.3	300	2.7	IHI	1999–2002
8	South district of Nagoya University, 4th line, high speed transit, Nagoya, Japan	Subway	Clay, sandy silt, sandy gravel	∅6.52 × W11.12	876	11.5–21.3	200	3.1	IHI	1999–2002
9	Yagoto north district, 4th line, high speed transit, Nagoya, Japan	Subway	Clay, sandy gravel	∅6.52 × W11.12	782	19.0–24.0	180	0.9	KHI	1999–2002
10	Yamashitadori south district, 4th line, high speed transit, Nagoya, Japan	Subway	Sandy gravel	∅6.52 × W11.12	957	10.0–16.6	165	3.3	MHI	1999–2003
11	Yagoto south district 4th line, high speed transit, Nagoya, Japan	Subway	Clay, sandy gravel	∅6.52 × W11.12	1025	16.2	300	3.1	MHI	1999–2003
12	East-terrain line, 1st district, Aichi, Japan	Subway	Sandy soil	∅6.73 × W11.43	904	7.0–15.0	102	5.9	IHI	NA
13	East-terrain line, Aichi, Japan	Subway	Clay, sand	∅6.73 × W11.43	123	12.0–13.0	102	0	IHI	NA
14	Nenjiang Rd. St. to Xiangyin Rd. St. to Huangxing greenbelt St., line 8 Shanghai Metro, China	Subway	Silty sand, silty clay, clayey silt	∅6.52 × W11.12	1759	5.2–12.0	495	2.8	IHI	2003–2004
15	Kairu Rd. St. to Nenjiang Rd. St., line 8, Shanghai Metro, China	Subway			929	5.2–12.0	495	2.8	MHI	2003–2004
16	Lot 9, line 6, Shanghai Metro, China	Subway			1713	4.0–21.0	300	2.7	IHI	2004–2005
17	Lot 10, line 6, Shanghai Metro, China	Subway			2497	6.0–13.0	990	1.5	IHI	2004–2005
18	Lot 11, line 6, Shanghai Metro, China	Subway			1096	6.0–10.0	420	2.7	IHI	2004–2006
19	Lot 10, line 3, Shanghai Metro, China	Subway			1459	12.3–19.8	NA	NA	IHI	~2009
20	Lot CA450A,Taoyuau International Airport Access MRT, Taiwan	MRT	Silty clay, silty sand	∅6.42 × W11.62	1584	7.6–26.0	280	4.9	IHI	2009–2010

of view, limited information regarding the construction cost and duration for both single-circular and DOT shield tunneling methods was reported in the literature. In this article, the speed and duration of DOT shield tunneling for the construction of TIAA MRT were collected and compared with values suggested by Shield Tunneling Association of Japan (2004). A comparison of tunneling cost between single-circular twin-tube and DOT shield tunneling was also made.

2. DOT shield tunneling in Taipei basin

The objective of Taoyuan International Airport Access MRT is to provide airport passengers with a safe, convenient, comfortable and high quality transit service. TIAA MRT system between Taipei and Jhongli will link the Taoyuan International Airport to the Taiwan High Speed Rail (HSR), Taiwan railway systems, and Taipei MRT systems. The total budget for this project is approximately US$ 3.56 billion.

As illustrated in Fig. 1, the project starts from Taipei Main Station (A1 Station), passes through Sanchong, Sinjhuang, Linkou, Taoyuan International Airport (A12–A14a Stations), and terminates at Jhongli Train Station (A21 Station). The route intersects Taiwan High Speed Rail at HSR Taoyuan Station (A18 Station). The total route length is 51.03 km, consisting of 10.92 km of underground section and 40.11 km of elevated section. In Fig. 1, the TIAA MRT system has 22 stations, consisting of 7 underground and 15 elevated stations. The expected revenue service date for entire system is October 2014.

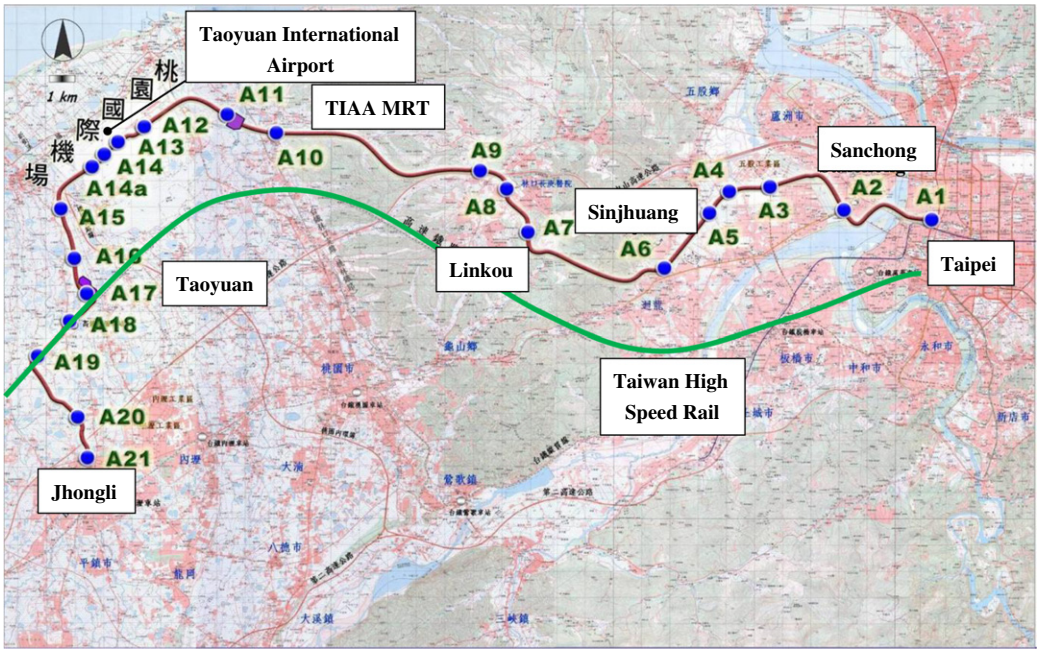

Fig. 1. Taoyuan International Airport Access MRT system.

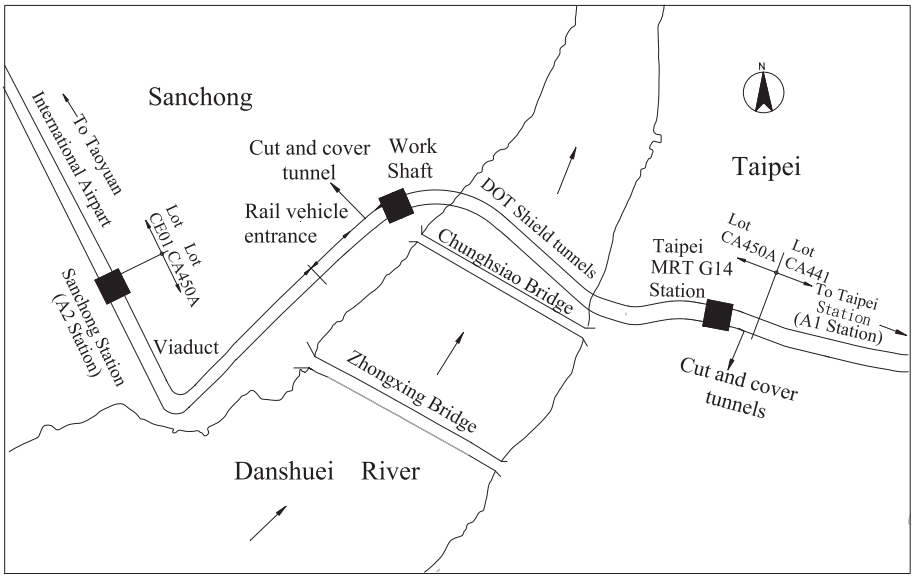

Fig. 2. Plan of lot CA450A between Taipei and Sanchong.

2.1. DOT tunneling from Sanchong to Taipei

The shield tunneling with DOT method from Sanchong to Taipei is introduced in this section. Fig. 2 shows that the lot CA450A is located between Station A2 of TIAA MRT and Station G14 of Taipei MRT, and the tunnel passes under Danshuei River. To avoid the difficulties and potential risks associated with the excavation of three cross-passages between two single-circular tunnels under Danshuei River, the DOT shield tunneling method was selected.

Excavation started from the work shaft at Sanchong, passed under Danshuei River, and terminated at G14 Station. As listed in Table 1, the total length of the DOT tunnel is 1584 m. The overburden above the tunnel varies from 7.6 to 26.0 m. The maximum tunnel slope is 4.9% and the minimum radius of curvature of the route is 280 m. The owner of the project is the Department of Rapid Transit Systems, Taipei City government, and the contractor is the Da-Cin/Shimizu joint venture.

2.2. Subsoil conditions

The DOT tunneling for lot CA450A was carried out in Taipei basin, which is an area of Quaternary Holocene alluvial deposits. Woo and Moh (1990) reported, in descending order, the alluvial deposits consist of a topsoil layer (1–6 m thick), the Sungshan Formation (40–70 m thick), the Chingmei Formation (0–140 m thick), and the Hsinchuang Formation (0–120 m thick). Most underground projects in Taipei were constructed less than 25.0 m below ground level; hence most construction works are carried out in the topsoil and the Sungshan Formation.

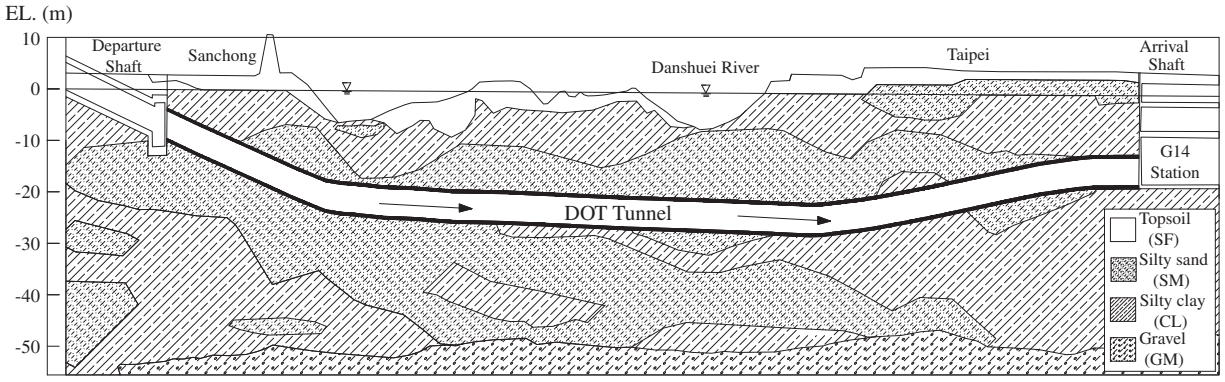

Fig. 3. Geological profile for tunneling.

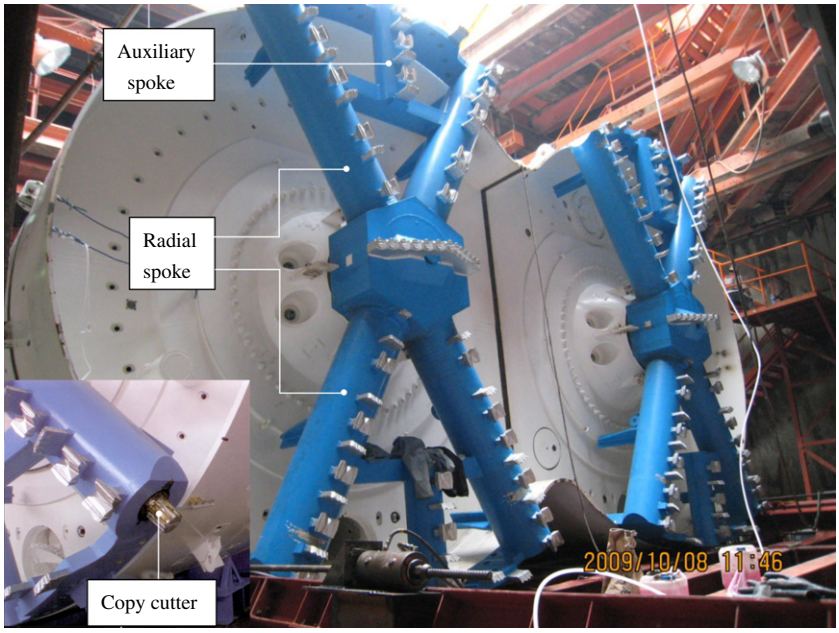

Fig. 4. Cutter heads of DOT shield machine.

Fig. 3 shows the geological profile interpreted from the site investigation for Contract CA450A (Da-Cin/Shimizu, 2009). In descending order, properties of the layers involved with this project are as follows:

(1) Layer 1 (Topsoil): A layer of surface fill (indicated as SF), located at 0 to 3.0 m below ground level, with Standard Penetration Test (SPT) *N*-value ranging from 1 to 5.
(2) Layer 2 (Sungshan Formation): Inter-layers of silty clay (classified as CL, $N = 4–7$) and silty sand (classified as SM, $N = 8–18$), located at 3–50 m below ground level. Traces of decayed wood, organic matter and shell fragments were reported.
(3) Layer 3 (Chingmei Formation): A layer of silty gravel (classified as GM, $N > 50$), located at about 50 m below ground level.

The ground water table was typically 2.9–5.0 m below ground level. It may be observed in Fig. 3 that DOT tunneling for lot CA450A was entirely carried out in the silty sand and silty clay layers of the Sungshan Formation.

2.3. DOT shield machine

The mud-injection Earth-Pressure-Balance (EPB) type DOT shield machine adapted for this project is shown in Fig. 4. This articulated shield machine was designed and manufactured by IHI, and has the outside dimensions of ∅6.42 m × W11.62 m. A total of 32 shield jacks were installed in the shield, including 20 upper jacks with 2000 kN capacity each, and 12 lower jacks with 2500 kN capacity each.

Fig. 4 shows two cutter heads were equipped in front of the DOT shield for soil excavation. Each cutter head has four radial spokes and two auxiliary spokes. The adjacent cutter heads rotate in opposite directions on the same plane. The motion of the two heads is synchronized for avoiding to touch or smash each other. Each cutter head is equipped with two copy cutters with the stroke of 150 mm. The copy cutter shown in Fig. 4 was used for overcutting of the ground at the curved section of tunneling, and also used for the correction of shield rolling. More information about cutter head of DOT machine may be found in Chow (2006).

Fig. 5 shows the cross sectional area of the DOT tunnel. Each ring of tunnel lining consists of 11 segments (8A + 1B + 1C + 1D),

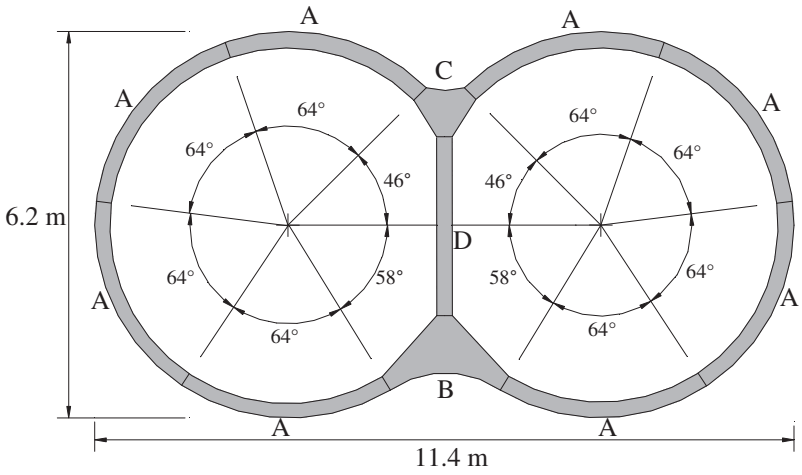

Fig. 5. Section of tunnel.

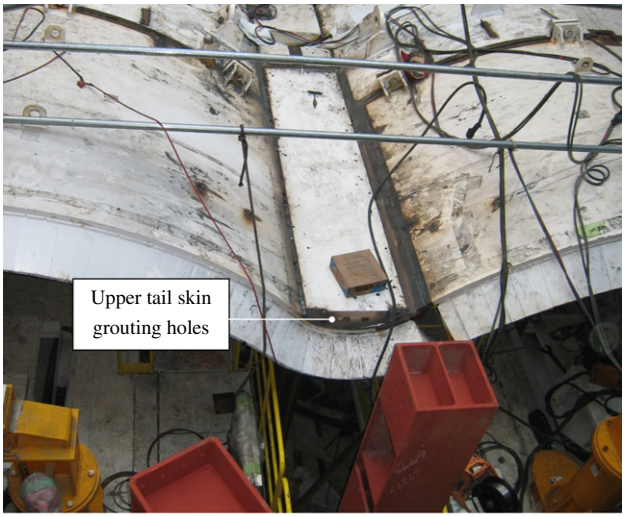

(a)

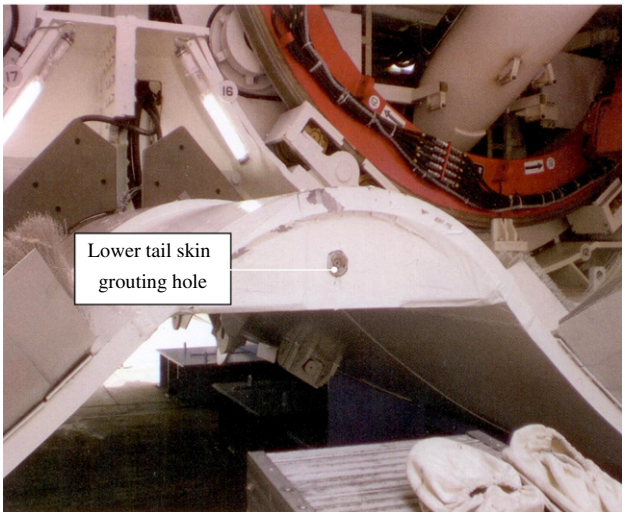

(b)

Fig. 6. Instantaneous backfill grouting holes.

and the segments are connected with straight steel bolts. Due to their size and shape, the segment B is often nicknamed the large seagull and segment C is nicknamed the small seagull. To avoid creating a continuous weak plane on the tunnel lining, the large and small seagulls swap their positions in the next ring. The reinforced concrete segments are 0.3 m thick and 1.2 m long. The assembled tunnel section is 11.4 m wide and 6.2 m high. The tail void of the DOT shield is 0.11 m thick. To reduce the ground settlement due to tail void closure, two grouting holes were fabricated above the upper seagull segment, and one grouting hole was fabricated below the lower seagull segment as shown in Fig. 6a and b. When the lining segments were pushed out of the shield, instantaneous grouting was automatically conducted to fill the newly generated tail void space. After the lining segment had been pushed out of the shield, backfill grouting was conducted manually through the grouting hole on the segment as shown in Fig. 7.

Fig. 8 shows the south portal of the DOT shield tunnel. Note in Fig. 8 that a flood-preventing gate was constructed at the entrance of the tunnel. The gate is used to isolate and protect the completed tunnel and DOT machine from a possible flooding problem in the work shaft during typhoon seasons. Fig. 9 shows the DOT shield tunnels for the construction of TIAA MRT. The passage between the two tunnels is used to establish an automatic fire-protection sliding door. In case of a fire emergency, the MRT passenger could escape from one tunnel to the other through the door.

2.4. Backfill grouting

The backfill grout material consisted of a mixture of grout A and grout B as indicated in Fig. 7. For every cubic meter of mixture, grout A consisted of 250 kg of cement, 30 kg of bentonite, 3 l of stabilizer, and 820 l of water. Grout B consisted of 85 l of water glass. The amount of grout used per ring was determined with the backfill injection rate, which is defined as follows:

$$\text{Backfill injection rate} = \frac{\text{Volume of grout injected per ring}}{\text{Volume of tail void per ring}} \times 100\% \quad (1)$$

For lot CA450A, the tail void area of the DOT shield was 3.45 m^2 and the length of the lining segment was 1.2 m. The volume of tail void per ring was 3.45 m^2 × 1.2 m = 4.14 m^3. The backfill injection rate was assigned to be 130%. As a result, the total volume of back-

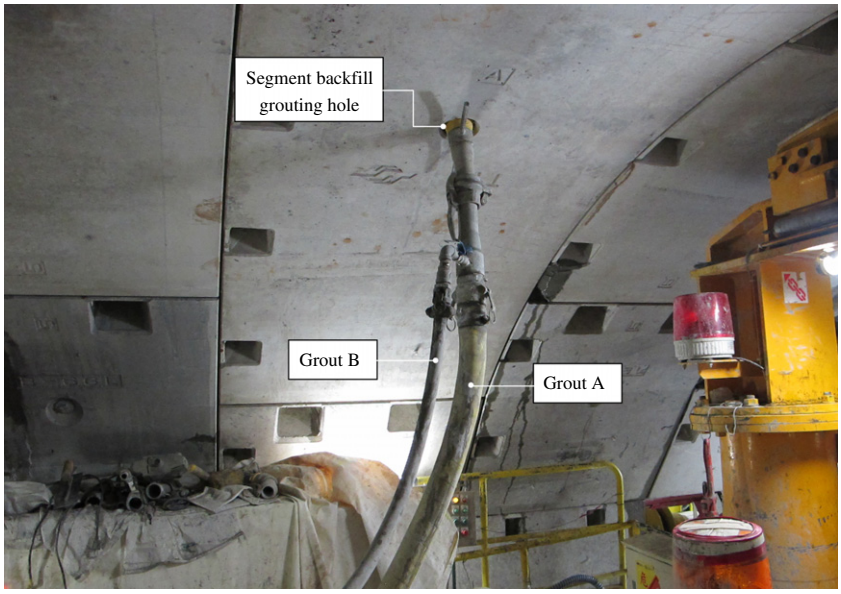

Fig. 7. Segment backfill grouting.

Fig. 8. South portal of DOT shield tunnel.

Fig. 9. DOT shield tunnels under construction.

fill injected at tail skin and segment grout holes was 5.38 m^3 per ring.

For the grout to fill the tail void successfully, the backfill pressure was controlled to be 100–200 kPa above ground water pressure. For example, at the monitored section of SSI-3 of lot CA450A, the tunnel center line was located at the depth of 20.85 m, and the ground water table was located at 2.9 m below ground level. The ground water pressure at the tunnel center line was 176 kPa. By adding 100–200 kPa to the water pressure, the backfill grouting pressure would be 276–376 kPa. The contractor used 200–400 kPa as the pressure range for both tail skin and segment backfill grouting. To prevent damaging the lining segments and connecting bolts, 400 kPa was selected as the upper bound value for backfill grouting pressure.

2.5. Face management

The excavated soils were mucked out of the tunnel with hydraulic pumps and pipes. Therefore, polymer slurry was injected at the face through the injection pipes on the cutter heads. Mud injection was carried out for the following reasons: (1) prevent soils sticking to the soil chamber; (2) enhance a plastic flow of excavated soils; and (3) reduce the applied torque due to soil-cutter friction.

The volume of mud injection at the face was determined with the assigned face injection rate. For the DOT shield used in lot CA450A, the cross-sectional area was 61.54 m^2 and the face injection rate was assigned to be 10%. For each ring, the volume of polymer slurry injected at the face was calculated by 61.54 $m^2 \times 1.2$ m $\times$ 10% = 7.38 m^3.

To keep the ground in a stable condition during tunneling, the EPB shield machine measured and controlled the lateral earth pressure in the soil chamber. The upper management earth pressure shown in Fig. 10 was calculated by adding 20 kPa to the earth pressure at-rest at the face. To prevent heaving of structures near the tunnel, the lower management earth pressure was determined by adding 20 kPa to the active earth pressure. In Fig. 10, the upper earth pressure changed form 110–332 kPa, and the lower pressure varied form 74–245 kPa.

The measured face support pressure was also indicted in Fig. 10. From ring 40 to 290, the DOT tunnel passed beneath an

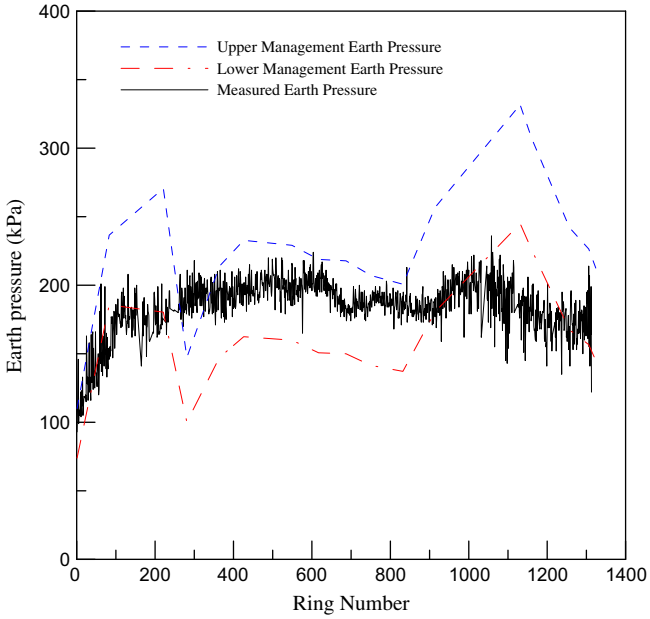

Fig. 10. Face support pressure.

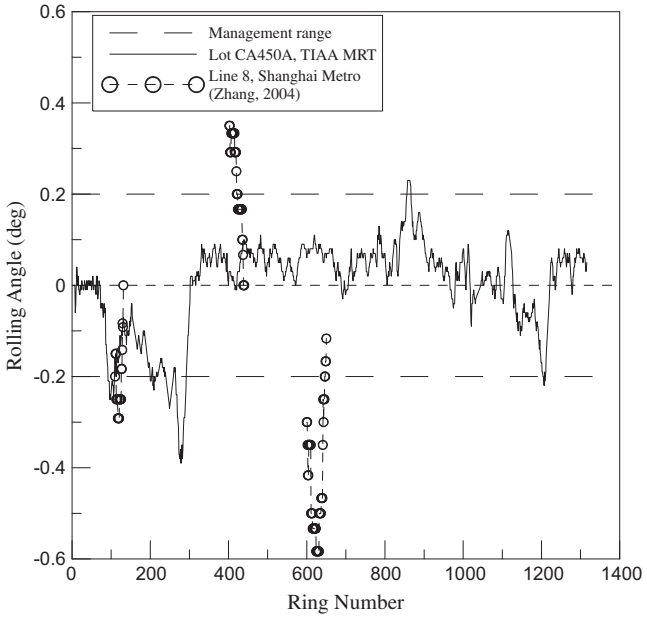

Fig. 11. Rolling angle with ring number.

underpinned bridge foundation. The face pressure was controlled to be less than the lower management value to avoid damaging the bridge foundation. From ring 991, the tunnels were driven under existing buildings. As a result, the face pressure was controlled below the lower management pressure.

2.6. Rolling of shield

During construction, rolling is one of the characteristics of the DOT shield machine. Main reasons of rolling include asymmetry of the cross section of the DOT shield due to manufacturing error, non-balanced weight of both sides of the DOT shield machine, and difference of torques of both cutter heads due to different soil properties. The reasons of rolling and their correction measures were summarized by Zhang (2004) and Shen et al. (2009).

In Fig. 5, assuming the tunnel rolls 0.5° clockwise with respect to its center, which is the center of segment D, the left tunnel would rise 22.7 mm and the right tunnel would settle 22.7 mm. The occurrence of shield rolling would cause a difference in elevation between two tunnels and a tilting of the center column of the lining segments. Shield rolling makes the distribution of internal forces among segments more complex and the lining assembly more difficult.

Fig. 11 shows the measured rolling angle of the DOT shield as a function of the ring number of the tunnel. Ring 1 was assembled on December 14, 2009. For an operator in the tunnel facing the excavation zone, a clockwise rolling angle is defined as positive. The management target of the rolling angle was between +0.2° and −0.2°. That means correction measures are required for a measured rolling angle more than plus or minus 0.2°. In the DOT tunnel design, for both TIAA MRT and Shanghai Metro, the limiting design rolling angles during construction are plus or minus 0.6°.

In Fig. 11, the rolling angle became significant at ring 117, the measured rolling angle was −0.29°. To reduce the amount of shield rolling, correction measures such as reverse-rotation of cutter heads and secondary grouting with opposite direction of rolling were carried out. The rolling angle was successfully reduced to −0.10° at ring 130. The maximum rolling angle −0.39° was measured at ring 278. The contractor employed reverse-rotation of cut-

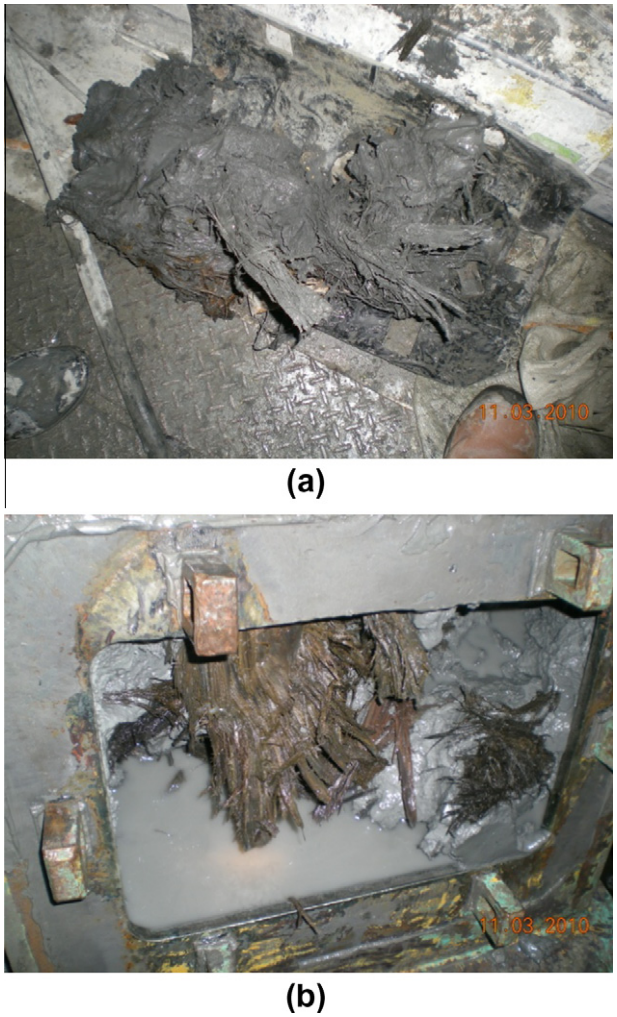

Fig. 12. Drift woods excavated by DOT shield.

ter heads, secondary grouting, and over-excavation by the copy cutter to reduce the amount of rolling to a small positive angle less than +0.10°. For a comparison, the rolling angle measured at line 8 of Shanghi Metro is also indicated in Fig. 11. It is clear in the figure that, throughout the tunneling of lot CA450A, the rolling angle was controlled by varying between +0.23° and −0.39° approximately, which was within the limiting values of +0.6° and −0.6° proposed by both TIAA MRT and Shanghai Metro.

2.7. Drift woods

In Taipei basin, drift woods had been a major problem for tunneling with single-circular shield machines. Taipei basin is covered with a 40–70 m-thick alluvial Sungshan Formation. Large-size tree trunks were encountered in the alluvial stratum during underground excavation for MRT stations and building basements. Ju et al. (2009) reported, during shield tunneling for Banqiao Line lot CP261 of Taipei MRT, a 0.9 m-long 0.3 m-diameter drift-wood piece was recovered in the soil chamber of an EPB shield. For the next 40 m of tunnel excavation for lot CP261, drift woods were encountered for 10 times.

As seen in the Fig. 2, the DOT shield was used for excavation under Danshuei River. It is highly possible that drift woods could be encountered in the alluvial riverbed. For lot CA450A, Fig. 4 shows different types of steel cutting-bits were attached to spokes of the cutter heads. It is expected that large pieces of drift wood could be chopped off by the cutting-bits to small pieces and then mucked out. For this project, drift woods were frequently encountered during tunneling. Clogging of the screw conveyor due to drift woods during excavation was reported. Manual removal of the clogged drift-wood pieces from the screw conveyor was conducted and tunnel excavation was successfully completed. Fig. 12a and b show the drift wood pieces excavated by the DOT shield.

3. Settlement due to DOT tunneling

In this section, formations of ground settlement troughs due to DOT shield tunneling measured in the field are reported. Since there are only 20 cases of DOT tunneling in the world up to 2010, the settlement data available are limited. In this study, six sets of surface settlement data recorded in Tokyo, Shanghai and Taipei were collected and studied. Only surface settlement is discussed in this paper. Based on the findings of Peck (1969), the empirical equal-area method and superposition method are briefly introduced and used to estimate the surface subsidence due to DOT shield excavation. On the basis of experience gained through field measurements, the empirical method provides simple and practical alternatives to numerical solutions.

3.1. Peck's method

Based on field data, Peck (1969) suggested that the surface settlement trough over a single circular tunnel can usually be approximated by the error function or normal probability curve as follows:

$$S(y) = S_{\max} \times \exp\left(\frac{-y^2}{2i^2}\right) \tag{2}$$

where $S(y)$ is the settlement at offset distance y from the tunnel center line (tunnel axis), $S_{\max}$ is the maximum settlement above tunnel center line, and i is the distance from the inflection point of the trough to the center line. The parameter i is commonly used to represent the width of the settlement trough. Peck presented a dimensionless relationship between the width of settlement trough i/R versus depth of tunnel $Z/2R$ for tunnels driven through different materials, where R is the radius of the tunnel, and Z is the center line depth. Based on error function, the maximum surface settlement $S_{\max}$ and the volume of surface settlement trough per linear length V_s has the following relationship:

$$V_s = \sqrt{2\pi} i S_{\max} \approx 2.5 i S_{\max} \tag{3}$$

Ground loss due to tunneling is defined as:

$$\text{Ground loss} = \frac{V_s}{V_t} \times 100\% \tag{4}$$

where V_t is the volume of tunnel excavated per linear length.

3.2. Equal area method

In Fig. 13, Zhang (2007) suggested that the ground settlement due to DOT shield tunneling can be approximated with that due to a single-circular tunnel which has the same cross-sectional area as the DOT tunnel. The volume of settlement trough per linear length due to DOT tunneling $V_{s,DOT}$ can be monitored in the field. The volume of settlement trough per linear length due to the single-circular tunnel with a radius R_{eq} is assumed to be equal to $V_{s,DOT}$.

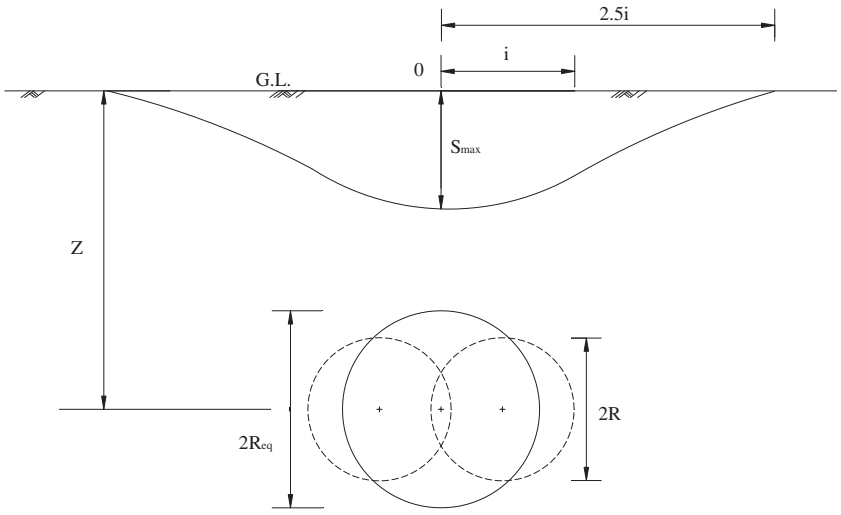

Fig. 13. Ground settlement due to a single circular tunnel with equal area.

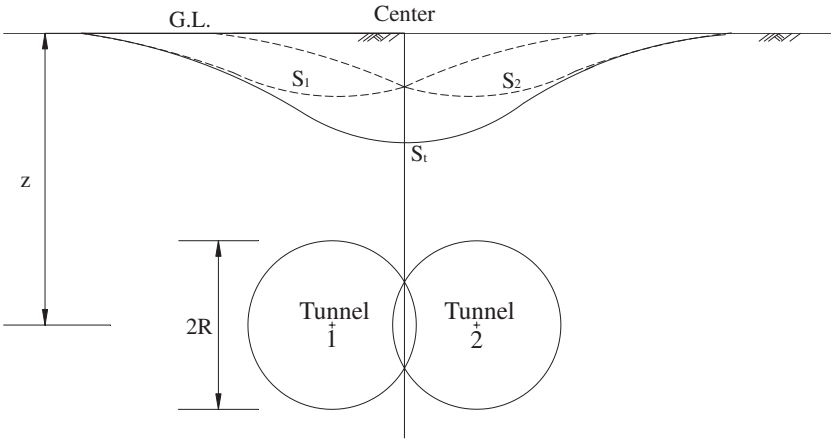

Fig. 14. Superposition of ground settlement due to two single-circular tunnels.

The next step is to determine the ground settlement curve due to the single-circular tunnel with a radius R_{eq}. In Eq. (3), with the volume of settlement trough $V_{s,DOT}$ monitored in the field and the trough width parameter i determined with the dimensionless relationship proposed by Peck, the maximum surface settlement S_{max} can be obtained. By substitute S_{max} and i into Eq. (2), the distribution of settlement due to the tunneling of an equal-area single-circular shield can be calculated. This settlement trough is assumed to be equal to that due to DOT shield tunneling.

Assuming the single circular tunnel with a radius R_{eq} has the same cross-section area as the DOT tunnel. For each linear length of tunnel driving, exactly the same volume of soil would be excavated by the single circular tunnel and the DOT tunnel. This is the reason why the settlement trough was assumed to be equal.

3.3. Superposition method

For a pair of parallel tunnels, if the interaction between the tunnels can be neglected, Fang et al. (1994) suggested that principle of superposition may be used to estimate ground subsidence associated with the construction of parallel tunnels. In Fig. 14, the settlement distribution due to the construction of tunnel 1 and 2 is illustrated as curve $S_1(y)$ and $S_2(y)$, respectively. The total settlement $S_t(y)$ due to the two circular tunnels is calculated with the principle of superposition: $S_t(y) = S_1(y) + S_2(y)$.

Due to symmetry, it is assumed that each single-circular tunnel would share 50% of the total ground loss. That means the volume of settlement trough induced by each circular tunnel was assumed to equal $0.5V_{s,DOT}$. For each circular tunnel, the trough width parameter i could be determined with the dimensionless relationship proposed by Peck. The maximum surface settlement S_{max} for each tunnel could be obtained with Eq. (3), and the settlement distribution curve S_1 and S_2 for each circular tunnel could be calculated with Eq. (2). The total settlement curve S_t is the summation of settlement curves S_1 and S_2.

It should be mentioned that the displacements and strains associated with tunneling will always create a disturbed zone surrounding the tunnel. Hoyaux and Ladanyi (1970) analyzed the stress distribution surrounding tunnels driven through soft soils with the finite element method. Their finding indicated that, among many other factors, the width of the plastic zone is mainly influenced by the sensitivity of the soil deposit and the diameter and depth of the tunnel. It is quite obvious that many assumptions and uncertainties are involved in the proposed empirical methods.

3.4. Settlement troughs monitored in the field

Six settlement troughs monitored at Ariakekita common conduit in Tokyo, Shanghai Metro, and Taoyuan International Airport Access MRT are illustrated in Fig. 15a–f. For comparison purposes, the settlement curves estimated with the empirical equal-area and superposition methods are also included in these figures.

The ground settlement data due to tunneling for Ariakekita common conduct are shown in Fig. 15a. Oda and Yonei (1993) reported the DOT shield driven through clay and gravel deposits was 9.36 m-diameter and 15.86 m-wide. At the monitoring section, the depth of tunnel center-line was 20.68 m and the induced ground loss was 0.23%. This was the smallest ground loss among the six settlement troughs reported in Fig. 15. The maximum settlement estimated with the equal-area method was greater than the field data.

The surface movements monitored at the 80th ring, line 8 of Shanghai Metro are presented in Fig. 15b. Zhou et al. (2005) reported ground heaving was observed due to the earth-pressure-balance shield tunneling. The settlement data monitored at the 460th ring, Line 8, of Shanghai Metro are presented in Fig. 15c. The ground loss induced by DOT tunneling was 0.67%. Field data in Fig. 15c exhibit a narrow and W-shaped settlement trough, which is quite different from all other measured settlement curves shown in Fig. 15, and those estimated with the empirical methods.

Fig. 15d shows the settlement trough recorded at the 100th ring, lot 9, line 6 of Shanghai Metro. The field settlement data are in fairly good agreement with settlement curves estimated with both empirical methods. A similar finding could be observed in Fig. 15e.

The settlement trough measured at SSI-3 section, lot CA450A of Taoyuan International Airport Access MRT is shown in Fig. 15f. The measured settlement trough was not symmetric. The monitored settlement trough was wider than the estimated troughs, and the monitored maximum settlement was apparently smaller than the estimated values. The ground loss due to DOT tunneling was 1.30%, which is the largest one among the six values reported in this study.

In Fig. 15, the ground loss due to DOT shield tunneling varied from 0.23% to 1.30%, and the average ground loss was 0.78%. Based on field data, Chang (2007) reported that, for a single-circular EPB shield machine tunneling through cohesive soils, the induced ground loss varied from 0.12% to 7.48%. It may be concluded that, as compared to that due to single-circular EPB shield tunneling, the range of ground loss due to DOT shield tunneling would be narrow,

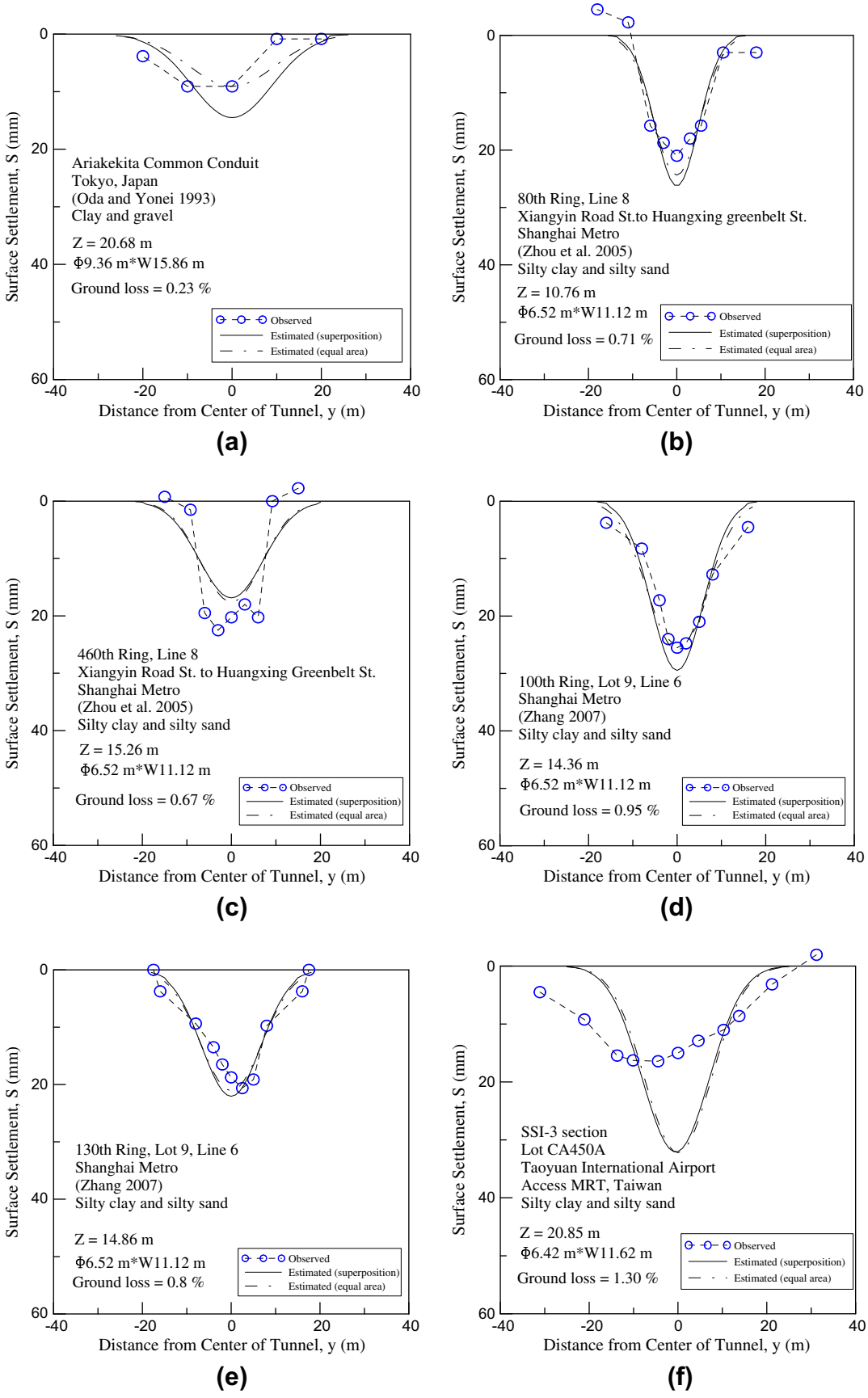

Fig. 15. Measured vs. estimated settlement trough due to DOT shield excavation.

and the peak ground loss value would be significantly less. Except the segment backfill grouting, Fig. 6 shows instantaneous grouting was conducted at the upper and lower skin-tail grouting holes. The tail void space generated when the lining segments were pushed out of the shield was backfilled automatically and instantaneously. This is probably the main reason why the ground loss due to DOT shield tunneling was lower.

4. Duration and cost of DOT tunneling

Duration, cost, quality and safety of construction are the four major factors considered for civil engineering projects. In this section, the duration and cost of DOT shield tunneling for the construction of lot CA450A of Taoyuan International Airport Access MRT are reported.

4.1. DOT tunneling duration

The speed of shield tunneling is mainly influenced by the tunnel diameter ($2R$), tunneling slope, radius of curvature (r) of alignment, initial or normal stage of excavation, and subsoil conditions. The Shield Tunneling Association of Japan (2004) reported the tunneling speed decreases with increasing tunnel diameter. As illustrated in Fig. 16, for the DOT shield with a diameter $2R = 2.35$ m, the normal-stage (300 m < r, nearly a straight-line) tunneling speed is 7.6 m/day. For a larger DOT shield with the diameter $2R = 9.2$ m, the normal-stage tunneling speed is reduced to 5.1 m/day. It is also reported the tunnel speed in the initial-excavation stage is only about 50% of that in the normal stage. The tunneling speed for initial-stage excavation as a function of tunnel diameter is also indicated in Fig. 16.

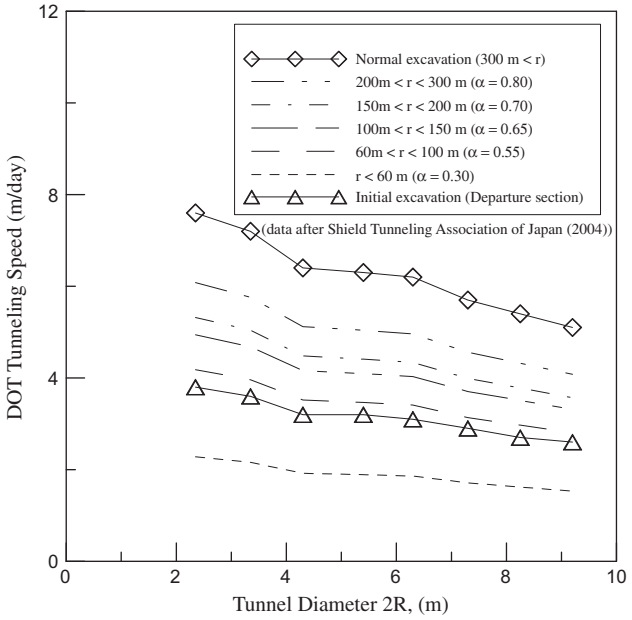

Fig. 16. DOT tunneling speed with tunnel diameter 2R and radius of curvature r.

The Shield Tunneling Association of Japan (2004) reported that tunneling speed would slow down for excavation along curved alignment. The tunneling speed for curved excavation L_c (m/day) can be evaluated with the following equation:

$$L_c = \alpha \times L_s \tag{5}$$

where L_s is the tunneling speed in normal-stage (straight line portion), and α is the reduction factor. The variation of α factor as a function of the radius of curvature r of tunnel alignment is indicated in Fig. 16. If the radius of curvature is greater than 300 m, α is equal to 1.0. If the radius of curvature is less than 60 m, the tunneling speed at the sharp turn is only 30% of that for the straight-line portion. In Fig. 16, the tunneling speed is expressed as a function tunnel diameter, radius of curvature, and initial or normal-stage of advancing.

Fig. 5 shows, for lot CA450A of TIAA MRT, the DOT tunnel has a diameter of 6.2 m. In Fig. 13, the corresponding straight-line normal-stage tunneling speed $L_s = 6.2$ m/day. The minimum radius of curvature is 280 m, and the associated reduction factor $\alpha = 0.8$. Based on Eq. (5), the tunnel speed in the curved portion is approximately $L_c = 4.96$ m/day. Assuming the tunneling crew works 25 days per month (30 days), the tunneling speed would be 4.1 m per calendar day. However, Fig. 2 indicates the middle and final portions of the tunnel are not curved, thus the tunneling speed for the normal-stage excavation was estimated to be about 4.3 m/day as indicated in Table 2.

For the initial and final stages of excavation, the tunneling speed was reduced 50% from 6.2 m/day down to 3.1 m/day. A steep 4.9% downhill slope was encountered at the initial stage of excavation, and the expected tunneling speed was further reduced to 2.4 m/day. Assuming the tunneling crew works 25 days per month, the tunneling speed for the initial-stage becomes 2.0 m each calendar day as listed in Table 2.

A comparison of tunneling duration for the construction for lot CA450A with both the single-circular twin-tube and DOT shield tunneling methods are summarized in Table 2. With the DOT shield, it is expected to take 400 days to complete the tunneling assignment. In the table, since the assembly of the circular lining segments is less complicated, it is estimated to take only 273 days to construct the twin-tunnels with the single-circular shield machines.

The DOT tunneling for lot CA450A stared on December 11, 2009 and it was completed on December 5, 2010. For the initial stage, the measured tunneling speed 2.5 m/day was slightly faster than the estimated speed 2.0 m/day. For the normal-stage, the actual tunneling speed 4.55 m/day was also faster than the expected

Table 2
Comparison of tunneling speed and duration.

Tunneling method	Item	Departure section	Normal excavation	Arrival section	Total
Single-circular twin-tube tunneling(estimated)	Tunnel length (m)	60	1464	60	1584
	Tunneling speed (m/day)	2.5	6.5	2.5	4.9
	Duration of construction (day)	24	225	24	273
DOT shield tunneling (estimated)	Tunnel length (m)	60	1464	60	1584
	Tunneling speed (m/day)	2.0	4.3	2.0	4.0
	Duration of construction (day)	30	340	30	400
DOT shield tunneling (measured)	Tunnel length (m)	60	1464	60	1584
	Tunneling speed (m/day)	2.5	4.55	4.3	4.4
	Duration of construction (day)	24	322	14	360

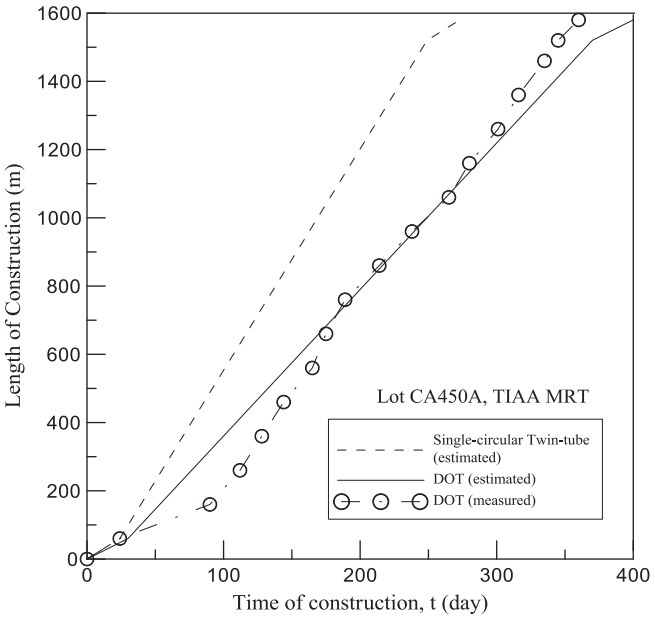

Fig. 17. Duration of DOT tunnel construction.

speed 4.3 m/day. As a result, the actual duration of tunneling was 360 days, which was 40 days shorter than the estimated duration.

The length of completed tunnel as a function of the time of construction is shown in Fig. 17. In the first 200 days of construction, the slower tunneling speed was most probable due to the initial steep downhill-slope of tunneling, small radius of curvature, and inexperience of the tunneling crew. After the first 200 days, most difficulties had been overcome and the crew became more skillful. The tunneling speed increased and the duration of construction was reduced. As compared with single-circular twin-tube tunneling method, underground excavation with the DOT method would increase the tunneling duration for about 32%.

4.2. DOT tunneling cost

The cost of DOT shield tunneling for lot CA450A is presented in this section. Since this was the first time that DOT shield tunneling was conducted in Taiwan, the owner of the project asked five experienced Japanese contractors to evaluate the cost of DOT tunneling in Taipei. Table 3 shows the cost per meter of DOT tunneling proposed by the five contractors varies from US$ 19,520 to 42,330. On the average, each meter of DOT tunnel would cost US$ 28,810. Note that the tunneling cost listed in Table 3 was only valid in Taiwan in 2008.

For comparison purposes, the cost of construction of single-circular twin-tube shield tunneling is also listed in Table 3. The cost per meter of tunneling varied from US$ 14,710 to 23,230. The average cost per meter of tunneling was US$ 18,890. It may be concluded from Table 3 that the cost per meter of tunnel constructed with a DOT shield is about 1.5 times that constructed with single-circular shields. Department of Rapid Transit Systems (2008) reported that the DOT shield machine alone would cost US$ 10.57 million, which consists of 23% of the total tunneling cost. The DOT tunnel lining segments would cost US$ 24.2 million, which is about 53% of the total tunneling cost. The expensive DOT shield machine and the complicated manufacturing and assembly of DOT lining segments are the main reasons for the higher cost of tunneling.

Department of Rapid Transit Systems (2008) stated, based on the tunneling experience in Japan, the cost for DOT tunneling is about 1.3 times that for single-circular twin-tube shield tunneling. For the tunneling of lot CA450A in Taiwan, the DOT shield machine was constructed and transported from Japan, Japanese engineers and technicians would cost more to operate in a foreign country, and the lining segment molds and associated construction parts were used only for this project. These were the reasons why the cost of tunneling for lot CA450A of TIAA MRT was higher. However, it would cost a lot more budget and it would be much more risky to excavate three cross-passages between the single-circular tunnels under the river.

5. Conclusions

Based on the DOT shield tunneling for lot CN450A of Taoyuan International Airport Access MRT, the following conclusions can be drawn. Throughout the tunneling operation, the measured rolling angle of the DOT shield was controlled to vary between +0.23° and −0.39°, which were within the limiting design range of ±0.6° proposed by both TIAA MRT and Shanghai Metro.

For the six surface settlement troughs collected from Tokyo, Shanghai and Taipei, the ground loss due to DOT shield tunneling varied form 0.23–1.30%, and the average ground loss was 0.78%. As compared with the ground loss due to single-circular EPB shield tunneling, the range of ground loss due to DOT shield tunneling was relatively narrow, and the peak ground loss value was significantly less.

At the initial stage of excavation, the measured tunneling speed 2.5 m/day was faster than the estimated speed 2.0 m/day. At the normal-stage, the actual tunneling speed 4.55 m/day was also slightly faster than the expected value 4.3 m/day. As a result, the actual tunneling duration of 360 days was 40 days shorter than the estimated 400 days. As compared with single-circular twin-tube tunneling method, underground excavation with the DOT method would increase the tunneling duration for about 32%.

The cost per meter of tunnel constructed with a DOT shield was about 1.5 times that constructed with single-circular shields. The cost of shield machine and segment lining were 23% and 53% of the total tunneling costs respectively. The expensive DOT shield machine and the complicated manufacturing and assembly of lining segments are the main reasons for the higher cost of tunneling. However, it would cost a lot more budget and it would be much more risky to excavate three cross-passages between the single-circular tunnels under the river.

Table 3
Comparison of proposed tunneling cost (after Department of Rapid Transit Systems, 2008).

Contractor		D	K	N	O	S	Average
Cost per meter of tunnel × 10^3 (US$)	Single-circular twin-tube	21.10	20.13	15.29	23.23	14.71	18.89
	DOT shield	27.24	28.50	42.33	26.45	19.52	28.81

Acknowledgements

The authors thank Mr. Pei-Jeen Wu and Mr. Chien-Hsu Chen, North District Project Office, Department of Rapid Transit Systems, Taipei City Government, for providing valuable information and support. The assistance of Mr. Heng-Tzu Lin, CECI Engineering Consultants is gratefully acknowledged. Special Thanks are extended to Mr. Min-Yi Huang, NCTU for his kind assistance.

References

Chang, H.C., 2007. An Empirical Evaluation of Ground Settlement due to Shield Tunneling. Master Thesis, National Chiao Tung University, Hsinchu, Taiwan (in Chinese).

Chow, B., 2006. Double-O-tube shield tunneling technology in the Shanghai Rail Transit Project. Tunnelling and Underground Space Technology 21 (6), 594–601.

Da-Cin/Shimizu Joint Venture, 2009. Taiwan Taoyuan International Airport Access MRT Construction Plan – Lot CA450A Shield Tunnel Excavation Proposal (in Chinese).

Department of Rapid Transit Systems, Taipei City Government, 2008. Planning and Design of the DOT Tunnel of Taiwan Taoyuan Airport MRT Line. Civil Engineering Series, MRT Engineering Collection, vol. 30, 203 pp. (in Chinese).

Fang, Y.S., Lin, J.S., Su, C.S., 1994. An estimation of ground settlement due to shield tunnelling by the Peck–Fujita method. Canadian Geotechnical Journal 31 (3), 431–443.

Hoyaux, B., Ladanyi, B., 1970. Gravitational stress field around a tunnel in soft ground. Canadian Geotechnical Journal 7, 54–61.

Ju, D., Duann, S. W., Hwang, R., 2009. Influence of Drift Woods on Construction of Taipei MRT, Difficult Cases in MRT Geotechnical Engineering, Taiwan Geotechnical Society, pp. 424–429 (in Chinese).

Moriya, Y., 2000. Special shield tunneling methods in Japan. In: Proceedings of the International Conference on Tunnels and Underground Structures, Singapore, 26–29 November, pp. 249–254.

Oda, T., Yonei, I., 1993. Tunneling with large-section overlapping Double-O-Tube construction plan. Tunnels and Underground 24 (4), 39–46 (in Japanese).

Peck, R.B., 1969. Deep excavations and tunneling in soft ground: state-of-the-art report. In: Proceedings of the 7th International Conference on Soil Mechanics and Foundation Engineering, Mexico, City, pp. 225–290.

Shen, S.L., Horpibulsuk, S., Liao, S.M., Peng, F.L., 2009. Analysis of the behavior of DOT tunnel lining caused by rolling correction operation. Tunnelling and Underground Space Technology 24 (1), 84–90.

Shield Tunnelling Association of Japan, 2004. DOT Method's Excavation Speed, Appendix 7-2 and 7-3 (in Japanese).

Sterling, R.L., 1992. Developments in excavation technology, a comparison of Japan, the US and Europe. Tunnelling and Underground Space Technology 7 (3), 221–235.

Woo, S.M., Moh, Z.C., 1990. Geotechnical characteristics of soils in the Taipei basin. In: Proceedings of the 10th Southeast Asian Geotechnical Conference, Taipei, vol. 2, pp. 51–65.

Zhang, J., 2004. Cause of the Shield Machine Rolling and Correction Method during DOT shield Construction, Shanghai Tunnel, No. 3, pp. 8-27–8-30 (in Chinese).

Zhang, T.L., 2007. Research on the Ground Movement Induced by the Disturbance of Multi-circular Shield Construction and its Control Technology. Master Thesis, Tongji University, Shanghi, China (in Chinese).

Zhou, W., Wu, W., Gu, C., 2005. DOT shield driving technology applied in running tunnel project for Shanghi Metro. In: Proceedings of the 3rd Japan–China Technological Exchange of Shield-driven Tunneling in 2005, Waseda University, Japan, pp. 269–276 (in Chinese).